City Research Online

City, University of London Institutional Repository

This is the accepted version of the paper.

This version of the publication may differ from the final published version.

Experimental study and numerical analysis of progressive collapse resistance of composite frames

Lanhui Guo[1], Shan Gao[1], Feng Fu[2], Yuyin Wang[1]

1. School of Civil Engineering, Harbin Institute of Technology, Harbin 150090, China

2. School of Engineering and Mathematical Sciences, City University London, Northampton Square, London, EC1V 0HB, United Kingdom

Abstract: A partial damage caused by an abnormal load could trigger progressive collapse of high rise buildings which may lead to terrible casualties. However, in the process of column failure, "catenary action" plays an important role in redistributing the internal load and preventing progressive collapses of the structure. Rigid composite joints, thanks to their high strength and good ductility, exert great influence in catenary action. Therefore, an experiment related to a 1/3 scale progressive collapse resistance with the use of rigid composite joints was conducted, and the results of the experiment were analyzed. Based on the experiment results, a FE model was developed and analyzed. This paper describes the experiment, the results analyzed, and the FE model in detail. The experiment showed that the progressive collapse mechanism of composite frame consisted of 6 stages: elastic stage, elastic-plastic stage, arch stage, plastic stage, transient stage and catenary stage. In catenary stage, catenary action evidently enhanced the resistance to the progressive collapse of the frames. The steel-concrete composite frame with rigid connections designed in accordance to current design standards showed a good resistance to progressive collapse. It is also found that horizontal restraining stiffness of the frame exerted great influence on the resistance in catenary stage.

Keywords: composite structure; rigid joints; progressive collapse; catenary action; dynamic

Nomenclature	
E_s	Young's modulus of steel
F	Tie force
f_y	Yield strength of steel
f_u	Ultimate strength of steel
L	Length of beam

M_1	Sagging moment
M_{p1}	Plastic positive moment resistance
M_2	Hogging moment
M_{p2}	Plastic negative moment resistance
P	Vertical load
P_p	Plastic vertical resistance
Δ	Vertical displacement
θ	Rotation of joint

1. Introduction

Partial or full range progressive collapse of structures which is triggered by a local damage due to abnormal events such as gas explosion, bombing attack or vehicle collision may lead to terrible casualties and severe economic loss. It is mainly because that the loads on superstructures cannot be transferred downwards when a vertical load-carrying component fails. To prevent the progressive collapse of the structure, the internal force should be redistributed by Alternate Load Path, Tie Force [1-3], and especially the so called "catenary action". The resistance and ductility of the beam-to-column joints play an important role in the formation and performance of catenary action. The damage of joints may lead to the failure of forming catenary action, and then initiate the progressive collapse of the structures.

Compared with steel joints and reinforcement concrete (RC) joints, rigid composite joints consisting of steel beams and RC slabs exhibit a higher load-carrying capacity and better deformation ability [4-7]. Furthermore, the reinforcements in the RC slab are essential components contributing to "catenary action", especially when the steel joints do not satisfy the rotation demand of catenary action [8]. Therefore rigid composite joints are advantageous construction types of joints used in the system of preventing progressive collapses.

Since the collapse of Ronan Point of London in 1968, preventing progressive collapse of buildings has been recognized as an important design consideration. A series of design codes, standards and guidelines have been published, such as British Standard and Regulation[1-3], Eurocode[9-10], NBCC[11], ASCE7-05[12], ACI318[13], GSA2003[14], and DoD 2009[8]. In these codes and standards, there are two main design methods known as "direct design" and "indirect design". Direct design focuses on quantitative performance of structures while indirect design tends to prevent progressive collapse in the perspective of qualitative performance.

In recent years, there have been many analytical and numerical studies on progressive collapse analysis. Kaewkulchai and Williamson proposed a beam-column element formulation and solution procedure which can be used in dynamic analysis [15]. Buscemi and Marjanishvili [16] proposed a concise methodology for evaluating the predisposition of a structure to progressive collapse, in which the pendulum analogy method was adopted in the paper. Their pendulum analogy method reduced the progressive collapse issue to a conventional dynamic problem. Khandelwal and EI-Tawil [17] used computational simulation to investigate catenary action in moment resisting steel frames accounting for hardening, softening and ductile fracture behavior of steel. Izzuddin *et al.* [18] developed a novel simplified framework and a new design-oriented methodology for progressive collapse assessment of multi-storey composite buildings. The methodology offers a practical means for assessing structural robustness at various levels of structural idealization. Lee *et al.* [19] proposed two nonlinear analysis methods to be used for a simplified but accurate evaluation of progressive collapse potential in welded steel moment frames. A collapse spectrum for a quick assessment of the maximum deformation demands in progressive collapse was established. Mohamed [20] investigated the implementation of UFC 4-023-23 to protect against progressive collapse of corner floor panels when their dimensions exceeded the damage limits. Fu [21] built a 3-D finite element model representing 20-storey composite building. The model displayed the overall behavior of the 20-storey building under a sudden loss of column and provided important information for the additional design guidance on progressive collapse. Li *et al.* [22] improved the current Tie Force (TF) method to take into account the important factors such as the load redistribution in three dimensions, dynamic effects and internal force correction. Iribarren *et al.* [23] investigated the influence of design and material parameters in the progressive collapse analysis of RC structures including reinforcement ratio and column removal time.

Some experimental tests have also been conducted under column-removal scenarios. Yi *et al.* **Error! Reference source not found.** conducted a 1/3 scaled progressive collapse test of a 3-story reinforced concrete frame building with 4-bay, simulating the load transmission process. The experimental results showed that the RC frame with middle column failed would go through 4 stages including elastic stage, elastic-plastic stage, plastic stage and catenary stage. Demonceau *et al.* [25] conducted a test simulating the loss of a column in a 2-D composite frame with semi-rigid connections. Horizontal brace was used to provide lateral restraint for the composite frame. The development of the catenary action in the frame was observed and the results confirmed the development of membrane force in the beams. Yang and Tan [26] conducted seven experimental tests on the performance of common types of bolted steel beam-column joints subjected to catenary action. In the test, the extremity of joints was

3

pinned which was a simplified boundary condition. This study provided the behavior and failure modes of different connections, including their abilities to deform in catenary action. Sadek *et al.*[27] conducted an experimental study of two steel joints and two reinforced concrete joints under monotonic vertical displacement of a center column. Portions of structural framing systems were designed as the boundary condition of the joints. The study provided insight into the behavior and failure modes of steel joints and concrete joints, including the development of catenary action. Oosterhof and Driver [28] conducted a series of experimental tests on common steel shear connections under a middle-column-removal scenario. Three types of shear connections were investigated in a test set-up capable of applying any independent combination of moment, shear and tension. The study examined the relative performance of three connection types, as well as the effects of connection geometry and loading states.

From above studies, it can be seen that, they were mainly focused on numerical and theoretical. Some experimental tests have been carried out to investigate the behavior of the steel joints and concrete joints under column-removal scenario recently. The joints in these tests were mostly installed into a simplified boundary condition, rather than in a frame level. In this way, only the behavior of the joint directly above the removal column was studied. In addition, few tests have been carried out to date on the progressive collapse behavior of composite joints. Composite joint possesses higher moment-resistance, which makes it widely used in steel and composite structures. To clearly investigate the behavior of rigid composite joints in frames during progressive collapse, in this paper, a pseudo-static experiment of a rigid beam-to-column connected composite frame under the loss of middle column was conducted. There is no extra lateral restraint for the frame which means the joints could be tested in a more practical boundary condition. The behavior of the frame was studied in detail, including not only the behavior of the joint directly above removal column, but also the joints adjacent to the removal column. In addition, a finite element simulation was also carried out to further study the capacity of the composite frames in resisting the progressive collapse. Based on the model, parametric studies were also performed.

2. Experimental program

2.1. Specimen design and fabrication

Based on the loading capacity of actuator and experimental setup, a 1-storey composite frame with 4-bay was designed and fabricated in 1/3-scale. The height of storey was 1.2 m, and the span was 2 m. Steel beams were fully welded to the flanges of steel column to make rigid connections. This is a typical rigid connection type with high moment resistance, high initial stiffness and fast track for construction. The cross sections of steel beam and column

were H200×100×5.5×8 and H200×200×8×12[H-overall depth (d) ×flange width (b_f) ×web thickness (t_w) × flange thickness (t_f)] respectively. The depth and width of RC slab were designed as 100 mm and 800 mm, respectively. The reinforcement mesh ratio for the RC slab was 0.85%. Longitudinal plane reinforcements with the diameter of 12 mm are placed in two layers with equal spacing along the width of the slab. Two layers of 8-mm-diameter plane bars are supplied as transverse reinforcement to prevent longitudinal splitting failure of the concrete slab. The design of the shear studs for the composite joints in the frame is based on the Chinese Code for Design of Steel Structures (GB 50017-2003) following full composite design assumption. The shear studs with diameter of 16 mm were welded to the steel beam with spacing of 100 mm. The strength of studs is 235MPa. Detailed dimension of the specimen is shown in Fig. 1. The middle column was not supported which is to simulate the loss of a column. Fig. 2 shows the casting process of the connections.

To determine the steel material properties, three coupons were cut from each structural steel member and rebar respectively. The tensile strength was tested in accordance with the Chinese standard GBJ2975(1982). The material properties are listed in Table 1, where f_y, f_u, E_s are steel yield stress, tensile strength and elastic modulus respectively. Concreting work was carried out in the laboratory of Harbin Institute of Technology. The non-absorbent plywood was used as bottom formwork and side shuttering. Casting of 150×150 mm cubes for strength test and 150×150×300 mm cylinder for Young's modulus were carried out at the same time. They were cured in similar conditions as the slab. The test of these concrete cubes was carried out in accordance with the Chinese standard GBJ81-85(1985). The average compressive strength of concrete cubes is 26.4MPa. The Young's modulus of concrete is 2.65×10^4 MPa .

2.2. Experimental setup

The experimental setup is illustrated in Fig. 3. To make a fixed supports, the bottom columns were welded to two base beams which were fixed on the ground. Behavior of the steel frame as well as the concrete slab during the test was monitored. One linear variable displacement transducers (LVDT) was placed vertically to measure the vertical displacement of middle column A, while four LVDTs were placed horizontally to measure the horizontal displacement of column A, B, D and E. The locations of LVDTs are shown in Fig. 3 (b). Uniaxial strain gauges were placed on the rebar of the RC slab and joints of steel frame. Strain gauge rosettes were placed at the ends of steel beams and columns. The locations of uniaxial strain gauges and strain gauge rosettes are shown in Fig. 4.

2.3. Loading procedure

A 500kN hydraulic jack installed at the top of middle column C was employed to apply vertical load in succession (see Fig. 3 (a)). Column C is not supported which is to simulate the loss of a column. A 1000kN load transducer was installed to measure the exact value of vertical loading. It is easy to observe and investigate the redistribution and transferring of internal force after the loss of middle column in the frame using this loading method. The load was applied in accordance with the Chinese code JGJ 101-96(1996). In elastic range, the vertical load was applied with a load increment of one-fifth of the calculated capacity of the specimen. After yielding was reached, displacement control method was adopted until the frame lost its load-bearing capacity.

3. Experimental observation

The initial behavior of the specimen was elastic without any evident change. When the load reached 30 kN, cracks at the top surface of the RC slab were first observed, which initiated the tips of the inner-side flanges of column B and D as shown in Fig. 5(b). When the vertical load reached 50 kN, the cracks adjacent to the exterior flanges of column B and D, appeared simultaneously at the top of the RC slab. At the position of 1/4 span to the exterior flanges of column B and D, some cracks were observed at the top of the RC slab when the load increased to 120 kN. Cracks at the bottom of slab were observed near the exterior flanges of column B and D when the load reached 190 kN as shown in Fig. 5(c). At 220 kN, the cracks (Fig. 5(d)), started at the tips of the flange of column C, appeared on the bottom of slab in the middle joint firstly. At the load of 273 kN, the flange and web of steel beams at the inner-side of column B and C tended to buckle as shown in Fig. 5(e) and meanwhile the vertical displacement of column C reached 45mm. After the load exceeded 275 kN, the vertical displacement of column C increased rapidly and the resistance of frame began to decrease. The cracks with width of almost less than 2 mm was observed at the top of RC slabs, mainly concentrated around column B and D. The cracks at the bottom of RC slab were intensely distributed around column C. There were few cracks observed in other area.

The displacement control method was adopted subsequently. When the vertical displacement of column C reached 100 mm, the vertical load decreased to 256 kN and then maintained at the same level. After the displacement exceeded 130 mm, the load began to increase. In this stage, crushing of the slab along both sides of flanges of column C was observed evidently (Fig. 5(f)). Crack at the top of RC slab surrounding column B and D continued to spread and some cracks penetrated deep through the concrete slab (Fig. 5(g)). As the displacement control loading progressed, the resistance of frame kept increasing and the RC slab continued to be crushed. On the slab near the inner side of column B and D, the length and amount of cracks both increased. As the test carrying on, there was a

6

slight change in crack pattern. A number of new cracks appeared in a parallel pattern rather than a diagonal one which inclined towards column flanges. Afterwards some diagonal cracks occurred successively on the slab in the mid-spans of B-C and C-D as shown in Fig. 5(h). After the vertical displacement of column C exceeded 350 mm, some debris of concrete at the bottom of slab near column C began to peel off while the flange and web of steel beam BC on the inner-side of column B buckled severely as shown in Fig. 5(i). At displacement of 443 mm, fracture of weld seam occurred at the tips of the bottom flange of steel beam BC connected to column C (see Fig. 6(a)) when the load reached 402 kN. Then the fracture expanded to most area of the web. Therefore the test had to be terminated.

The phenomena of frame after test are shown in Fig. 6. Due to the tie force produced by catenary action, the column B and D were obviously inclined inwards to column C. The inward inclination of column A and E was not as severe as those of internal columns as shown in Fig. 6(b). Severe buckling was observed in the bottom flange of steel beam BC and CD where the lateral torsional buckling of web was also observed. Slight tendency of buckling was also visible in the bottom flange of the steel beam near column B and column D as shown in Fig. 6(c). It is clear that the internal joints at column B and D were withstood hogging moment on both sides. The loss of load-bearing capacity of frame was initiated by the fracture of weld seam occurred at the tips of the bottom flange of steel beam in the left side of middle joint. The fracture of the weld seam subsequently resulted in the fracture of the bottom flange and the web of the steel beam in the left side of column C as shown in Fig. 6(d-e). Fig. 6(f-g) shows the failure phenomena of RC slab around column C. After the test, the width of crack around inner side of column B and D reached 10 mm, as shown in Fig. 6(h) and Fig. 6(i).

The crack pattern on the RC slabs after the test is shown in Fig. 7. The bold lines denote the main cracks with width over 5mm. Due to the symmetry of cracks pattern, only half of the structure is presented. In the span of B-C, some 45° diagonal cracks were observed on both sides of slabs. These diagonal cracks were caused by shear lag effect in composite beam. In the span of A-B, there were only 3 parallel cracks on the top of the slab at the position of 1/4-span to column B. One crack was observed at the bottom of slab near the inner side of flange of column A (also column E). Consequently, the sagging moment and tensional force of external joint and external beam AB were small. From this observation, it can be concluded that after the vertical load-bearing component failed, if the adjoining load-bearing components (beams, columns and joints) could sustain the additional loads through catenary action, the destruction, even damages, may not evidently propagate horizontally. So the key design measurement of preventing progressive collapse should focus on utilizing the catenary action and strengthening the key structural members which may initiate progressive collapse, as well as the adjoining members.

4. Results and discussions

4.1. Relationship of vertical displacement V.S. vertical load

Fig. 8 shows the load-vertical displacement relationship curve of middle column C where no support is provided. It can be seen that except the descending stage (after point F) due to unloading while testing was terminated, the curve in Fig. 8 consists of six stages: elastic stage, elastic-plastic stage, arch stage, plastic stage, transient stage and catenary stage. The part OA of the curve shows the first stage-"*elastic stage*". In this stage, the load-deflection relationship can be considered to be linear as the specimen is almost elastic and the deformation is small. When the load reaches 150 kN, the curve goes into the second stage-"*elastic-plastic stage*". In this stage, from point A to point B, the load begins to increase non-linearly with the increment of displacement, while the stiffness begins to decrease.

The third stage from point B to point C is named as "*Arch stage*", in which the curve presents a trend as arch. In this stage, the load increases with the increasing of vertical displacement of column C. However, after the reach of the peak point, the load decreases with the increasing of vertical displacement of column C. The load at point B and point C are equal. The peak value of 275 kN is defined as "*Peak resistance*" while the load value of 256 kN at point B and point C is defined as "*Plastic resistance*". The increase of resistance is caused by "Arch action" which refers to the characteristic of composite joints as shown in Fig. 9.

As the vertical load applying on the top of column C, the joint of column C is subjected to a sagging moment while the adjacent joints are subjected to hogging moments. The asymmetry of cross section of composite beam would result in the difference in elevation between rotation centers of joints withstanding sagging moment and hogging moment. Usually, the elevation of rotation center of joint withstanding sagging moment is higher than the joint withstanding hogging moment. Therefore, when the vertical load applies, "*arch action*" is formed by treating the rotation center of joint withstanding sagging moment as arch crown and the rotation center of joints withstanding hogging moment as arch spring. Similarly, "*arch action*" also exists in RC structures [18], which is because of the asymmetry of reinforcement distribution in RC beams.

Arch action is beneficial to the resistance of frame with column failure which would produce a higher resistance than the traditional plastic resistance. When the elevation of rotation centers becomes identical under vertical load, it means the end of "*arch stage*". It is worthy to note that "arch action" acts since the beginning of load application

8

which could be proved by the relationship between horizontal displacement and vertical displacement in latter paragraph.

The fourth stage from point C to point D is defined as "*plastic stage*", while plastic hinges are fully formed in the joint C and inner-side joints B and D. In this stage, the vertical displacement of column C rises from 97 mm to 157 mm, while the vertical load remains about 256 kN. As shown in Fig. 10, the plastic hinge action can be expressed as:

$$P\Delta = 2\theta M_1 + 2\theta M_2 \qquad (1)$$

Considering that the increment of plastic hinge rotation is easily obtained for the rigid-plastic mechanism as:

$$\theta = \Delta / L \qquad (2)$$

Using Eqs.(1) and (2), the load P can be expressed as:

$$P = 2(M_1 + M_2)/L \qquad (3)$$

The positive plastic moment resistance (M_{p1}) and negative moment resistance (M_{p2}) of the rigid composite joint in the frame are 134 kN·m and 87 kN·m respectively , which are worked out according to the Chinese Code for Design of Steel Structures (GB50017-2010). Substituting M_{p1} and M_{p2} into Eq.(3), the plastic resistance P_p obtained is 246 kN which corresponds closely to the experimental result 256 kN.

Beyond Point D, the vertical load rises with the increasing of vertical displacement, and then the frame goes into the fifth stage DE named "*transient stage*". In this stage, the load rises with the increase of vertical displacement. The load-bearing mechanism of frame is in state of transition from "plastic hinge action" to "catenary action".

And then, the stiffness of the frame has a slight decline which means that the frame enters the final stage EF named "*catenary stage*". In this stage, "plastic hinge action" has faded due to the loss of moment capacity in middle joint of column C and inner-side joints of column B and column D. The vertical load is sustained by "catenary action" as shown in Fig. 11. Reinforcement in slab and steel beam withstand tensional force caused by catenary action together. The stiffness of the frame in this stage is slightly lower than that in "transient stage". But substantially, the load increases linearly with the increase of vertical deflection.

"*Ultimate resistance*" is defined as the maximum resistance of frame before the collapse happens. The ultimate resistance observed is 402 kN, which is 1.5 times higher than *peak resistance* and 1.6 times higher than *plastic resistance*. The corresponding ultimate vertical displacement is 443 mm, 8 times bigger than peak displacement correspondent to *peak resistance*. It can be concluded that the steel-concrete composite frame designed with current design standards and specifications provides sufficient capability of preventing progressive collapse and good deformation ability.

4.2.   Relationship curves of horizontal displacement V.S. vertical displacement

Fig. 12 shows the relationship curves of vertical displacement of column C V.S. horizontal displacements of column A, B, D and E. Deformation towards to column C is defined as positive value. The vertical lines refer to the vertical displacement of the stages from point A to point F of the curve shown in Fig. 8. The bold vertical line refers to the vertical displacement at peak resistance. As shown in Fig. 12, in the early stage of loading, the horizontal displacement of each column is negative value which means all the column deform outwards from column C. This phenomenon illustrates the "*arch action*" present in Fig. 8 and also proves that "*arch action*" does work at the beginning of load application. After the vertical deflection reaches the displacement corresponding to *peak resistance*, the horizontal deformation becomes to be positive value. The maximum negative value of horizontal deformation observed is -0.74 mm. Each column begins to move towards column C. When "*arch stag*e" ends at point C as shown in Fig. 8, each column substantially returns to the original position while the horizontal displacement of the columns is zero. Subsequently, following the increment of vertical deformation, the horizontal deformation of the columns continues to increase until the frame losses its bearing capacity.

The maximum horizontal displacement observed in column B and column D is about 36 mm, while the value of column A and column E is about 33 mm. The horizontal displacement of internal column B and column D is larger than external column A and column E all through the loading process, especially when the "transient stage" starts. This is because the joints B and D are subjected to hogging moment and tensional force caused by "catenary action" simultaneously while the joints of column A and column E mainly sustain tensional force.

4.3.   Measurements of strain gauges

Fig. 13 shows the strain distribution on steel beams and reinforcements before the vertical load reaches "peak resistance" (275 kN). The detailed location of strain gauges can be found in Fig. 4. The joints at position 1 and position 2 withstand the largest sagging moment and hogging moment respectively. As shown in Fig. 13(b-e), before the vertical load reaches 150 kN (referring to the point A in Fig. 8), the strain on the cross section of composite beam is small. Using the strain values, the stress on the beam can be calculated. It is found that the steel is still in elastic stage. At position 1, the neutral axis in the elastic stage is located in top flange of steel beam. When the vertical load reaches 250 kN, the steel beam yields, while the reinforcements in compression zone of slab are still in elastic stage. At position 2, the neutral axis of elastic stage is located at the 150 mm near bottom flange. When the vertical load reaches 250 kN, all reinforcements in the slab and parts of cross section of steel beam yield in tension and compression. The joint at position 3(Fig. 13(f) - Fig. 13(g)) is under hogging moment which is much smaller than

that of the joint at position 2. The cross section of composite beam remains in elastic stage until the load reached 275 kN. Fig. 13(h) - Fig. 13(i) show that the joint at position 4 is subjected to a hogging moment until the load reaches 275 kN. It proves that column A inclines slightly outward from column C due to "arch action". The hogging moment at position 4 is much smaller than that of joints at position 2 and position 3.

4.4.   Simplified Analysis model

Based on the test results, a simplified analysis model was developed in this section. When a column is lost in a frame, the frame can be divided into two parts: the directly affected part (DAP) and the indirectly affected part (IAP). DAP represents the part of the building which is directly affected by the loss of the columns. IAP represents the part of the building which is affected by the forces developing within and influenced by the directly affected part. As shown in Fig 14, the specimen in the test above could be divided into DAP and IAP.

The indirectly affected part in Fig.14 consists of two columns and a composite beam. They could be simplified as a horizontal restrained spring restraining the directly affected part. The stiffness of horizontal springs depends on bending rigidity of steel columns. Normally, the initial stiffness and moment resistance of composite joint under hogging moment is smaller than those under sagging moment. So the composite joints under hogging moment could be considered as rotational restrained springs. The stiffness of rotational springs depends on bending rigidity of composite joints under hogging moment. Consequently, the 4-span specimen could be simplified as a double-span composite beam with horizontal and rotation restrained springs as shown in Fig.15.

In elastic stage, vertical load is resisted in joints by bending actions. Horizontal restrained springs are not involved in this stage. The mechanics model in this stage could be considered as a double-span beam with rotational restrained springs as shown in Fig.16(a). With applying the vertical load, plastic hinges are formed in the middle or two ends of the beam as shown in Fig.16(b). When arch stage starts, plastic hinges have already formed in the middle and end of the beam as shown in Fig.16(c). Arch action produces a wave to the P- Δ curve which should be flat in this stage. In plastic stage when the arch action fades, the vertical displacement increases continually. The transient stage follows the plastic stage when the horizontal springs begin to participate in load resistance. In the transient stage, plastic hinge mechanism begins to transfer into catenary mechanism. The mechanical model of catenary stage is also shown as Fig.16(d). However in catenary stage, plastic hinges have transferred into tensional force and can not sustain bending moment anymore.

In arch stage, arch action would produce a higher resistance than the traditional plastic resistance. According to the analysis above, the veritcal load would come to its peak value when the horizontal displacemnt of arch spring

11

reaches the maximum. However, if the mechanical model shown in Fig.16(e) is adopted, the vertical load would be zero when the horizontal displacement of arch spring reaches the maximum. Based on this phenomenon, a new arch model with springs is proposed as shown in Fig.16(f). In this model, the bottom flange and part of web of steel beam are considered as tensional springs. The stiffness of the tensional springs depends on the involved area and length of steel beam. And the core zone of joint is considered as a incompressible bar to connect the arch and the spring members. In this model, the veritcal load would reach its peak value when the horizontal displacemnt of arch spring reaches the maximum. This model could be used to analyze the behavior of structure from elastic stage to arch stage.

5. Numerical analysis

5.1. Finite-element model

In addition to the experimental studies, Finite Element program ABAQUS is used to develop the numerical simulation of the test above. Steel components are simulated using beam elements (B31) while the slabs are simulated using the four-node shell elements (S4R) with bending and membrane stiffness. The reinforcement in the slabs is simulated with rebar-layer elements from the ABAQUS library as a smeared layer in the shell element. The structural beam elements are placed at the centerline of the structural beams and the shell elements are placed at the centerline of the slabs in the test. The beam elements and shell elements are coupled together using Tie command to simulate the composite action between the steel beams and RC slabs. The steel beam-to-column connections are modeled as rigid by connecting together directly. The finite element model is shown in Fig.17. It replicates the 1/3 scale test. The properties and dimensions of the model are identical to these of the specimen in the test.

The stress-strain relationship of steel is taken as bi-linear strength relationship considering stress hardening which in compression and tension are assumed to be the same. The harden rigidity after yield is equal to $1\%E_s$. The concrete damage plasticity model from ABAQUS is employed here to model concrete. The compressive yield curve is taken as that of a typical concrete from Chinese Code for Design of Concrete Structures (GB 50010-2010) Appendix C as shown in Fig.18. 10% of the compressive strength of concrete is considered as the tensile strength of concrete. The tensile strength of the concrete is 0.5 MPa after concrete cracking.

5.2. Model validation

The model was validated against the test results. Fig. 19 shows the comparison between calculated and experimental results. It can be seen that, good agreement is achieved in the initial stiffness, yield strength and the

12

behavior in latter stage (such as catenary action). Table 2 shows the detailed comparison between the results of test and simulation. The slope of the curve in catenary stage is defined as the stiffness of the structure in catenary stage. Due to the limitation of beam elements and shell elements in the terms of geometry simulation, the "arch action" in the experimental curve is not captured by the simulation curve. In the simulation curve, the structure goes into plastic stage after it yields. And there is no specific point to distinguish plastic stage and transient stage. But the points initiating "catenary stage" in the curves of test and simulation are close to each other. As overall behavior of the frame is more concerned, the model is accurate enough to conduct the progressive collapse analysis.

5.3. Dynamic column-removal analysis

Nonlinear dynamic time history technique is used here to simulate the scenarios of column removal. Column removal is conducted by element removal command which means the element representing the column would be deleted within a predefined time duration. The response of the structure is recorded in a dynamic analysis step. According to GSA [14], it is recommended that for the case where a dynamic analysis is performed, the vertical element should be removed over a time period which is no more than 1/10 of the period associated with the structural response mode for the vertical element removal. So the removal period is defined as 0.005 s. After the column removal is finished, a period of 2 s is added in the dynamic step subsequently to ensure the structure is stabilized.

According to the results of the experimental and static analysis, the plastic resistance of the remaining structure is 256 kN which is defined as the expected strength of the remaining structure (Q_{CE}). The load applied at the top of column C is defined as the demanded strength (Q_{UD}). So the demand-capacity ratio (DCR) is expressed as:

$$DCR = Q_{CE}/Q_{UD} \qquad (4)$$

Fig. 20 shows the influence of DCR on the behavior of the structure under the state of column removal. As shown in Fig. 20, with low DCR which means small vertical load at the top of column C, the vertical displacement of joint C reaches its first peak value at first and subsequently begins to vibrate after column is removed. It can be concluded that the structure remains in elastic stage and still exhibits good resilience. With the increase of DCR, the vibration of the joint C is weakened. When DCR is equal to 1.0, the remaining structure yield instantly and comes into the plastic stage with very small vibrations.

In order to compare the results of static analysis and dynamic analysis, based on the results of dynamic time history analysis, a pseudo-static curve is obtained in Fig. 21. On the pseudo-static curve representing the results of dynamic analysis, the value on Y-axis of each point represents the vertical load applied at the top of column C with different DCR, while the value on X-axis of each point represents the maximum displacement of each

dynamic-time-history curve in Fig. 20. The curve representing the result of static analysis also consists of six points with the value on Y-axis which is closed to these of the points on the pseudo-static curve.

In Fig. 21, the pseudo-static curve representing dynamic analysis consists of elastic stage, elastic-plastic stage and plastic stage, just as the static curve. The "plastic resistance" of the curve representing the result of dynamic analysis is almost the same as the result of static analysis. The vertical displacement of joint C in dynamic analysis is almost two times larger than that in static analysis under the same vertical load. It means that dynamic effect would not result in the decrease of resistance of remaining structure, but just increase the corresponding displacement. According to Fig. 21, the dynamic factor of vertical displacement is 2.0 for single storey composite frame.

5.4. Parametric studies

In order to investigate the factors affecting the behavior of the frame after column loss, three parameters were chosen for parametric studies which are rebar ratio (RR), height of column section (H_c) and height of steel beam section (H_b). The effects of these parameters on the behavior of frame after a column loss is analyzed via the vertical load-vertical displacement relationship curves.

5.3.1 *Influence of rebar ratio*

In this study, the rebar ratio of concrete slab varies from 0.6% to 1.1% (the value of 0.85% is adopted in the test). As seen in Fig. 22, rebar ratio does not influence the overall behavior of the remaining structure remarkably. The initial stiffness of the structures is identical. The increase of rebar ratio would enhance the hogging moment resistance of joint which subsequently increases the plastic resistance of the remaining frame. According to the experimental results, buckling of bottom flange of steel beam would restrict the contribution of reinforcement in the concrete slab. Even rebar ratio increases from 0.6% to 1.1%, the plastic resistance of the structure only increases by 4%. It can be concluded that the influence of rebar ratio in RC slab is not evident for progressive collapse resistance of composite frame. Table 3 shows detailed results of simulations with different rebar ratios. Although the plastic resistance of structures is increased by increasing the rebar ratio in slabs, the plastic displacement corresponding to plastic resistance is almost not changed.

5.3.2 *Influence of the depth of column section*

In this study, the depth of column section was chosen as 150 mm, 200 mm and 250 mm (the value of 200 mm is adopted in the test). The three column sections represent the section stiffness of $0.5K_c$, K_c and $2K_c$ respectively which are directly related to the horizontal restraining stiffness of the structure. As shown in Fig. 23, the initial

stiffness and plastic resistance of structures with different depth of column section are identical. Before reaching the vertical displacement of 160 mm corresponding to the end of plastic stage in the experimental curve (Fig. 8), the horizontal restraining stiffness has almost no influence on the elastic and plastic behavior of structures. After all plastic hinges have formed in the composite beams, the load-carrying mechanism begins to transform from plastic hinge action to catenary action when the horizontal restraining stiffness begins to influence the behavior of structures. With the increase of horizontal restraining stiffness, the stiffness of the structure in catenary stage increases remarkably, which consequently enhances the resistance of structure. The detailed results are shown in Table 4. All the data of simulations are the same, except for the stiffness of structure in catenary stage. When the depth of column section is increased from 150mm to 250mm, the stiffness in catenary stage is almost tripled. It could be concluded that high horizontal restraining stiffness is beneficial for the catenary action to carry and redistribute additional load.

5.3.3 *Influence of height of steel beam section*

The depth of steel beam section is chosen as 150 mm, 200 mm and 250 mm (the value of 200 mm is adopted in the test). The depth of the steel beam section is directly related to the initial stiffness, resistance of each stage and ductility of the structure. As shown in Fig. 24, the influence of H_b on the behavior of structures is remarkable. The structure adopting 150 mm-depth steel beam possesses lower initial stiffness and resistance than the other two. However, low stiffness ratio of beam-to-column brings a longer plastic stage which means better rotation capacity and ductility. Table 5 shows the detailed results. It is can be seen that the behavior of the structure is improved comprehensively, except for the stiffness in catenary stage which depends on the horizontal restrained stiffness.

6. Conclusions

In this paper, a steel-concrete composite frame with rigid beam-to-column connections was tested. The failure mechanism of the frame in the event of one column removal is studied in details. Based on the test, a FE model was developed and validated against the test results. Using the model, static parametric studies and dynamic column-removal analysis were conducted.

Based on the experimental and numerical analysis, following conclusions were made:

1. The collapse process of a rigid composite frame after one column removal consists of six stages: elastic stage, elastic-plastic stage, arch stage, plastic stage, transient stage and catenary stage. "Plastic hinge action" and "catenary action" play a major role in carrying load in early stage and late stage in preventing progressive collapse. The

steel-concrete composite frame designed with current Chinese design standards possesses good capability of preventing progressive collapse and shows good deformation ability.

2. "Catenary action" could enhance the resistance of rigid composite frame in progressive collapse evidently. The key design measurement in preventing the progressive collapse is the utilization of the catenary action and the enhancement of the key structural members which may initiate progressive collapse. "Arch action" is beneficial to the load-resistance of composite frame under column loss in early stage.

3. The increase of rebar ratio in slabs would not significantly enhance the resistance of the structure after column loss. The increase of depth of steel beam would improve the behavior of the structure dramatically Horizontal restraining stiffness has little influence on the behavior of the remaining structure before it begins to go into catenary stage. With the increase of horizontal restraining stiffness, the resistance of the remaining structure in catenary stage would increase remarkably.

Acknowledgements

References

[1]   Office of the Deputy Prime Minister. The building regulations 2000, part A, schedule 1:A3, disproportionate collapse. London (United Kingdom). 2004.

[2]   British Standard Institute. BS6399: loading for buildings, part 1: code of practice for dead and imposed loads. London (United Kingdom). 1996.

[3]   British Standard Institute. BS8110: structural use of concrete, part 1: code of practice for design and construction. United Kingdom. 1996.

[4]   European Committee for Standardization. EN 1994-1-1: 2003, Eurocode 4: design of composite steel and concrete structures. Part 1: general rules and rules for buildings. Brussels(Belgium). 2003.

[5]   Leon RT. Semi-rigid composite construction. Journal of Constructional Steel Research, 1990, 15(2):99-120.

[6]   Anderson D., Najafi AA. Performance of composite connections major axis end plate joints. Journal of Constructional Steel Research. 1994, 31(1):31-57.

[7]   Liew J.Y. Richard, Teo T.H., Shanmugam N.E., Yu C.H.. Testing of steel concrete composite connections and appraisal of results. Journal of Constructional Steel Research. 2000,56(2):117-150.

[8]   Department of Defense (DoD). Unified facilities criteria (UFC): design of structures to resist progressive collapse. Washington (DC). 2009.

[9]   European Committee for Standardization. EN 1991-1-7: 2006, Eurocode 1: actions on structures. Part 1-7: general actions-accidental actions. Brussels(Belgium). 2006.

[10] European Committee for Standardization. EN 1992-1-1: 2004, Eurocode 2: design of concrete structures. Part 1: general rules and rules for buildings. Brussels(Belgium). 2004.

[11] Canadian Commission on Building and fire Codes, National Research Council of Canada. National Building Code of Canada. Ottawa (Canada). 2005.

[12] American Society of Civil Engineers (ASCE). Minimum design loads for buildings and other structures (ASCE7-05). Reston (VA). 2005.

[13] American Concrete Institute (ACI). Building code requirements for structural concrete and commentary (ACI 318m-08). Detroit (Michigan). 2008.

[14] United States General Services Administration (GSA). Progressive collapse analysis and design guidelines for new federal office buildings and major modernization projects. Washington (DC). 2003.

[15] Kaewkulchai G., Williamson E.. Beam element formulation and solution procedure for dynamic progressive collapse analysis. Computers and Structures 82(2004):639-651.

[16] Buscemi N., Marjanishvili S.. SDOF model for progressive collapse analysis. Proceedings of the 2005 Structures Congress. ASCE. 2005.

[17] Khandelwal K., EI-Tawil S.. Collapse behavior of steel special moment resisting frame connections. Journal of structural engineering. 2007, 133(5):646-655.

[18] Izzuddin B.A., Vlassis A.G., Elghazouli A.Y., Nethercot D.A.. Progressive collapse of multi-storey buildings due to sudden column loss-Part 1: Simplified assessment framework. Engineering Structures, 2008,30(5)：1308-1318.

[19] Lee C.H., Seonwoong Kim, Han K.H., Lee K.. Simplified nonlinear progressive collapse analysis of welded steel moment frames. Journal of Constructional Steel Research, 65(2009):1130-1137.

[20] Mohamed O.. Assessment of progressive collapse potential in corner floor panels of reinforced concrete buildings. Engineering Structures, 31(2009):749-757.

[21] Fu F.. Progressive collapse analysis of high-rise building with 3-D finite element modeling method. Journal of Constructional steel research, 64(2009):1269-1278.

[22] Li Y., Lu X.Z., Guan H., Ye L.P.. An improved tie force method for progressive collapse resistance design of reinforced concrete frame structures. Engineering Structures, 33(2011):2931-2942.

[23] Iribarren S.B., Berke P., Bouillard Ph., Vantomme J., Massart T.J.. Investigation of the influence of design and material parameters in the progressive collapse analysis of RC structures. Engineering Structures, 33(2011):2805-2820.

[24] Yi W.J., He Q.F., Xiao Y. Collapse performance of RC frame structure. Journal of Building Structures. 2007, 28(5):104-117. (in Chinese)

[25] Demonceau J.F., Jaspart J.P. Experimental test simulating a column loss in a composite frame. Advanced Steel Construction, 6(3):891-913.

[26] Yang B., Tan K.H. Different types of steel joints under catenary action part 1: experimental tests. Proceeding of the Eurosteel 2011 Conference, Hungary.

[27] Sadek F., Main J.A., Lew H.S., Bao Y.H. Testing and analysis of steel and concrete beam-column assemblies under a column removal scenario. Journal of Structural Engineering, 9(2011):881-892

[28] Oosterhof S.A., Driver R.G. Performance of steel shear connections under combined moment, shear and tension. The Structures congress, 2012.
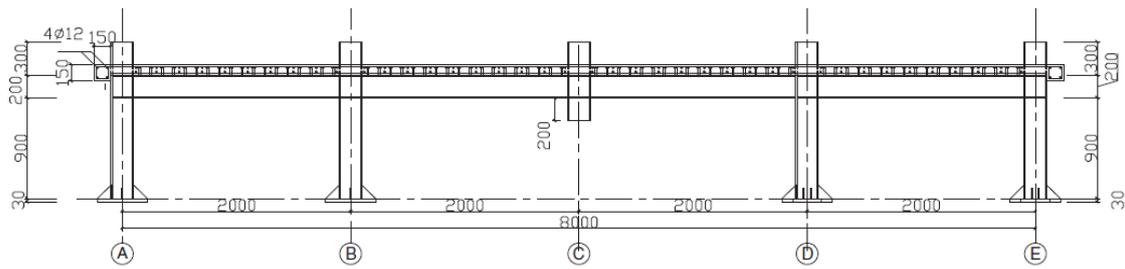
a) Detail dimension of frame (mm)
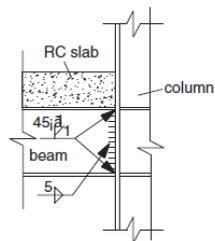
b) full-welded beam-to-column connection
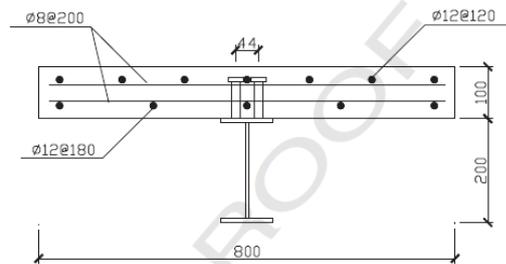
c) Cross section of composite beam

Fig. 1. Details and layout of frame.

a) Shear studs
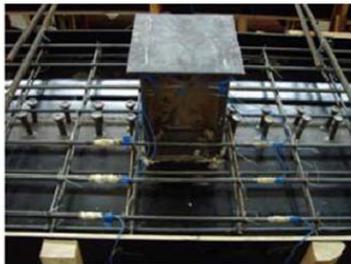
b) Reinforcement assembling

d) Concrete casting

Fig. 2. Fabrication of specimen.

a) Experimental set-up
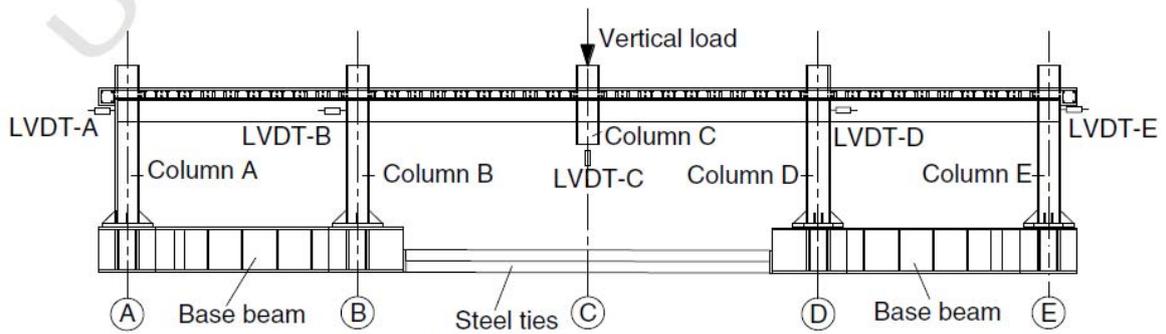
b) Distribution of LVDTs

Fig. 3. Experimental setup.
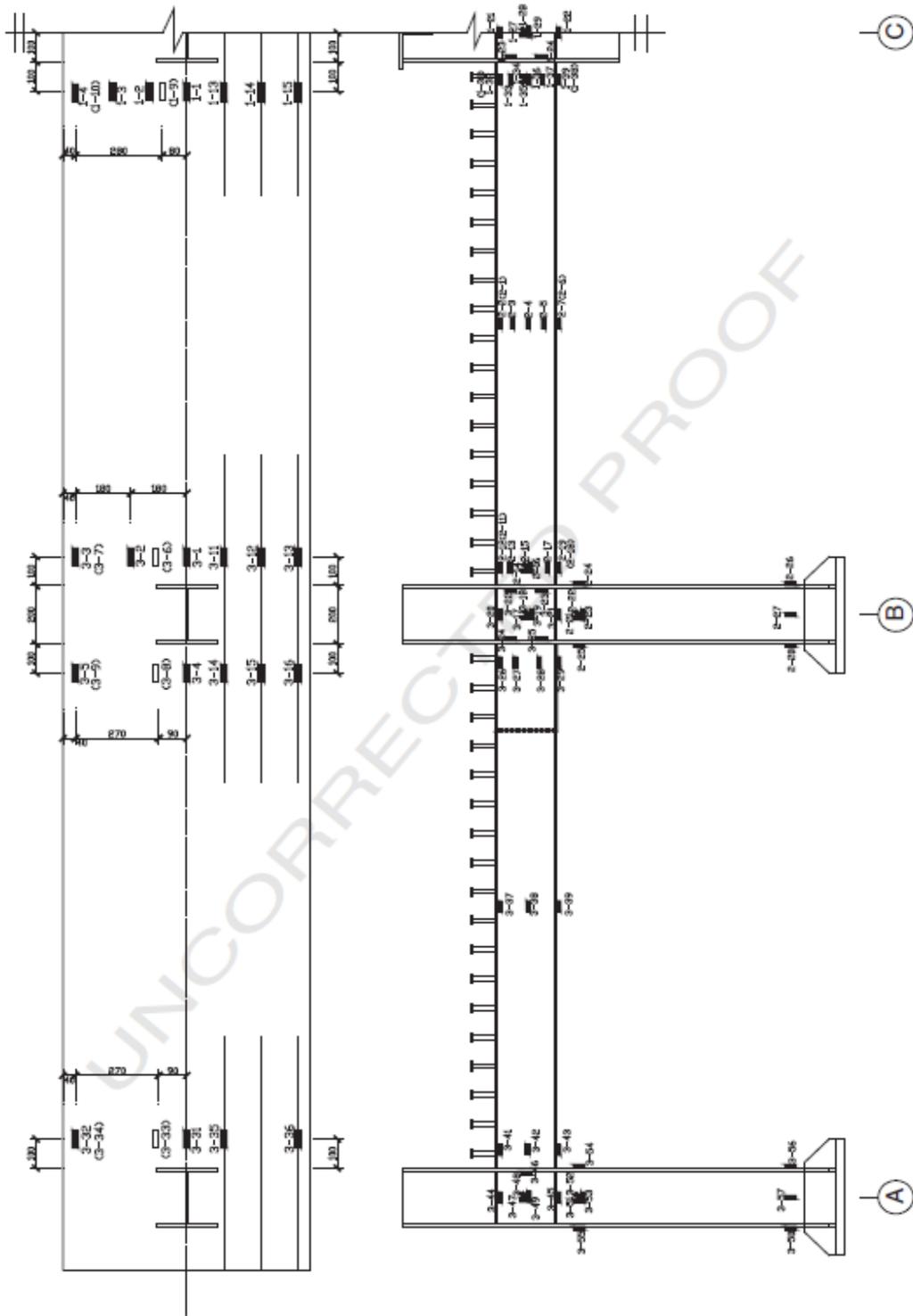
Fig. 4. Distribution of strain gauges and rosettes.
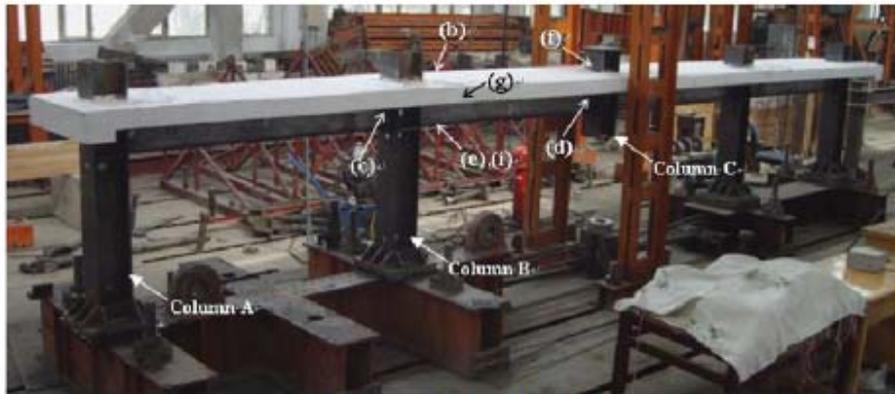
a) Positions of observation

b) First crack at the top of slab

c) First crack at the bottom of slab

d) First crack around column C
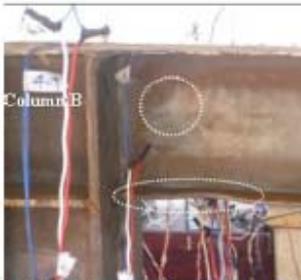
e) Initial buckling on the beam-end of BC

f) Crushing around column C
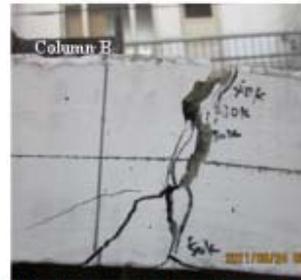
g) Cracks penetrating through slab

h) Diagonal cracks on the span of B-C

i) Severe buckling of beam flange near column B

Fig. 5. Phenomena of frame during experiment.

a) Overall experimental phenomenon

b) Inclination of column A and B

c) Buckling of beam in inside joint B

d) Fracture of weld seam in bottom flange

e) Tearing of the web of steel beam

f) Crack on the slab of middle joint

g) Buckling of reinforcement in slab

h) Crack on the slab of inside joint B

i) Details of inside joint B

Fig. 6. Phenomena of frame after experiment
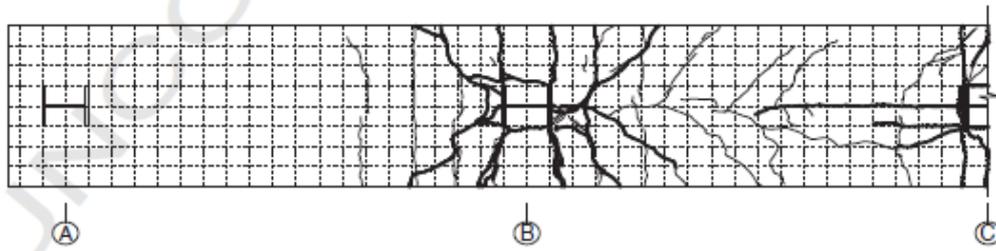
a) Crack distribution on the top surface of RC slab
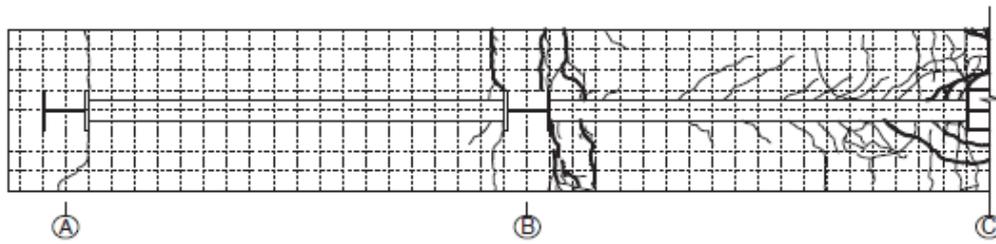
b) Crack distribution on the bottom bottom surface of RC slab

Fig. 7. Evolution of slab cracking in the span of A–B and B–C.

Fig. 4 Phenomena of frame after experiment
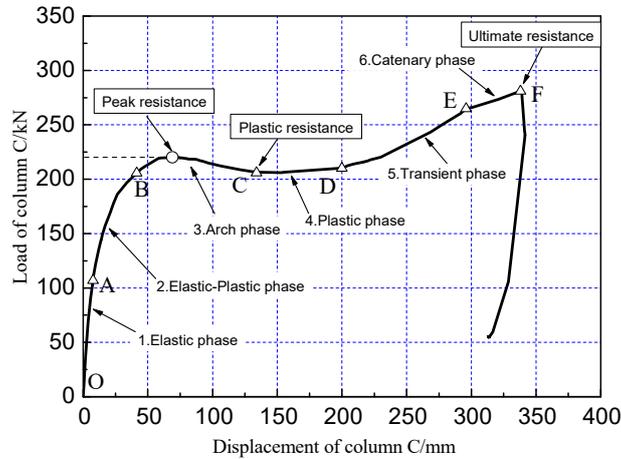
Fig. 8 Vertical load v.s. displacement of middle column relationship curve
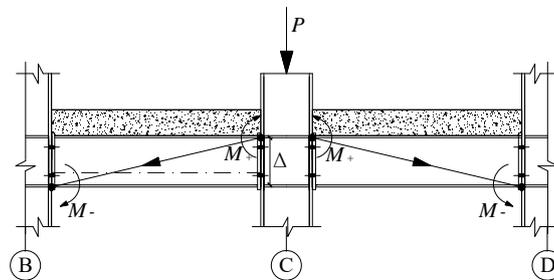

Fig. 9 Arch action
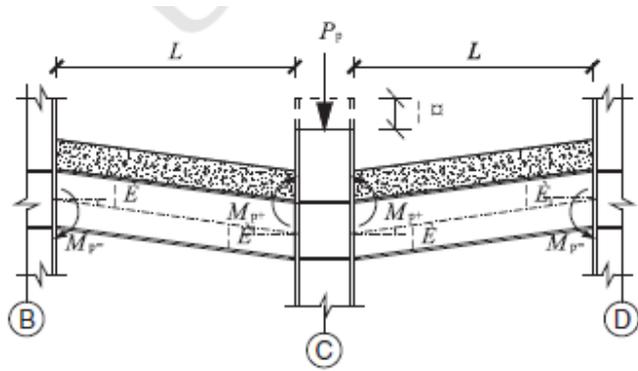
**Fig. 10.** Plastic hinge action.
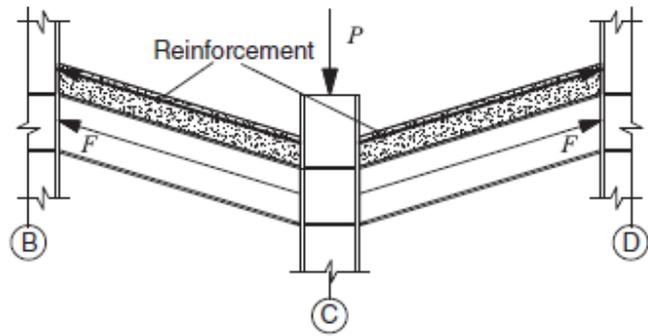
Fig. 11. Catenary action.
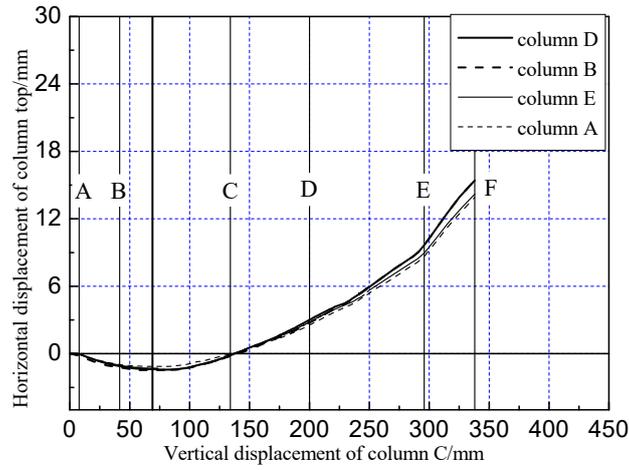
Fig. 12 Horizontal displacement of column top v.s. vertical displacement of middle column curves
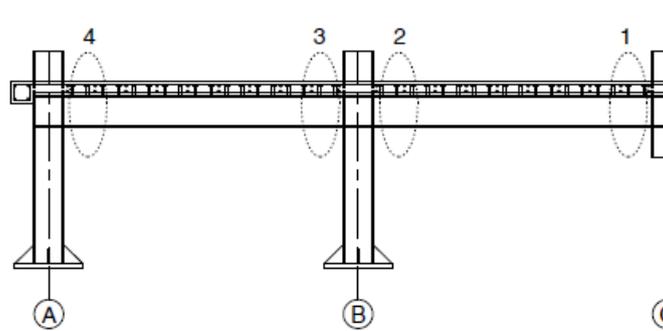

a) Positions of strain measurement
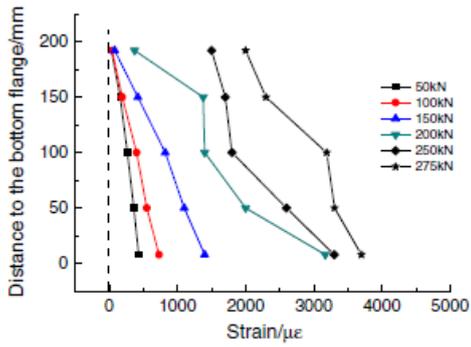
b) Strain along the height of steel beam at position 1

c) Strain of reinforcement at position 1

d) Strain along the height of steel beam at position 2

e) Strain of reinforcement at position 2

f) Strain along the height of steel beam at position 3
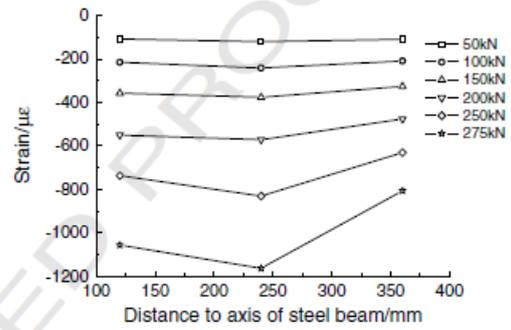
g) Strain of reinforcement at position 3
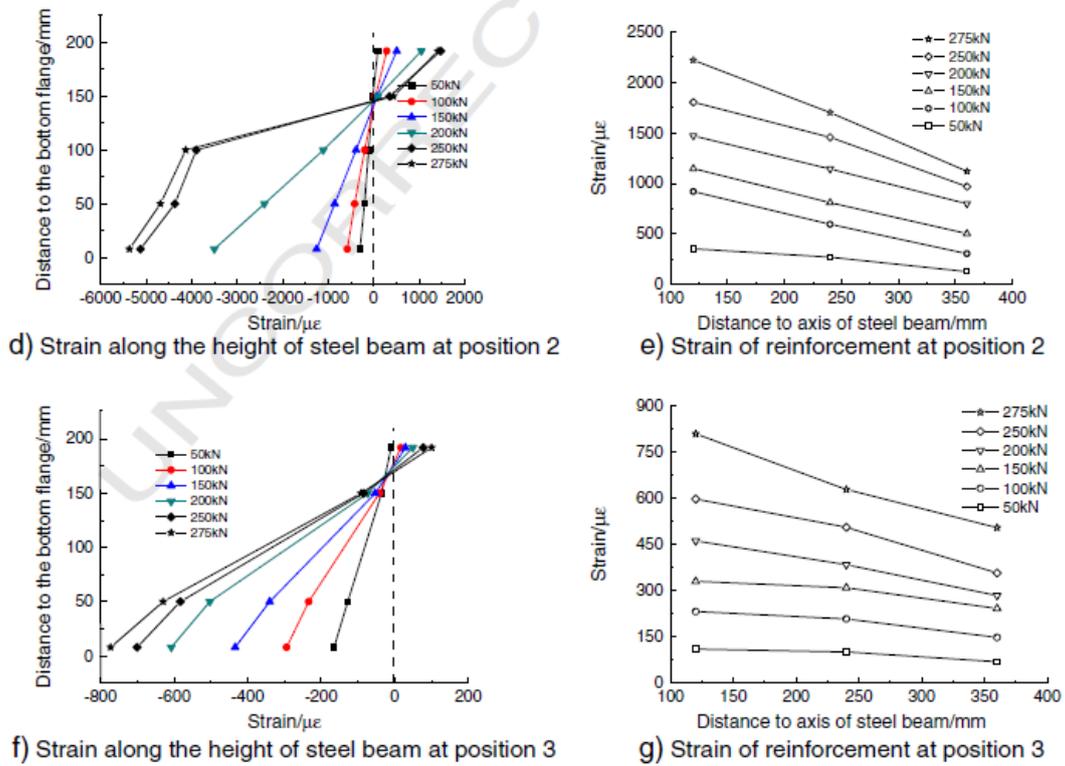
Fig. 13. Strain of steel and reinforcement.

h) Strain along the height of steel beam at position 4

i) Strain of reinforcement at position 4
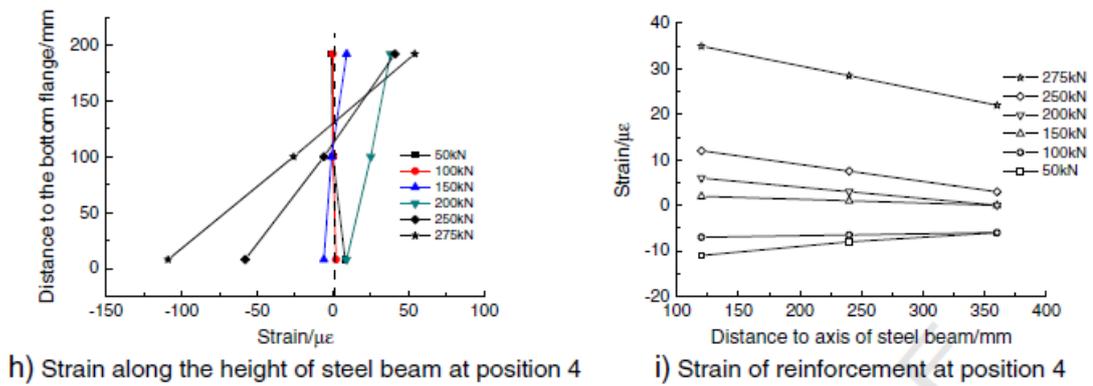
Fig. 13 (continued).

Fig. 7 Horizontal displacement of column top v.s. vertical displacement of middle column curves
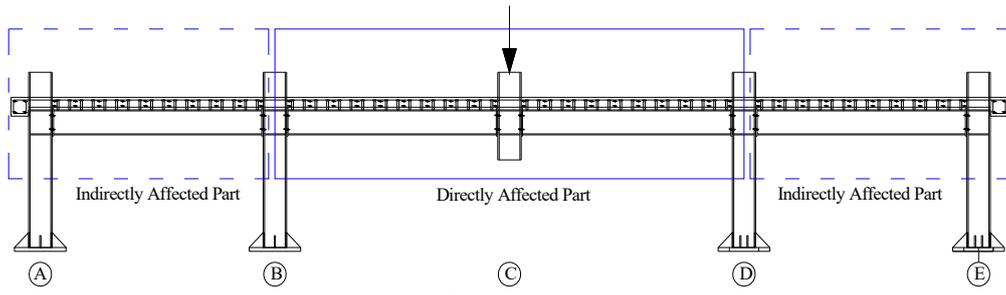
Fig. 14 Definition of DAP and IAP
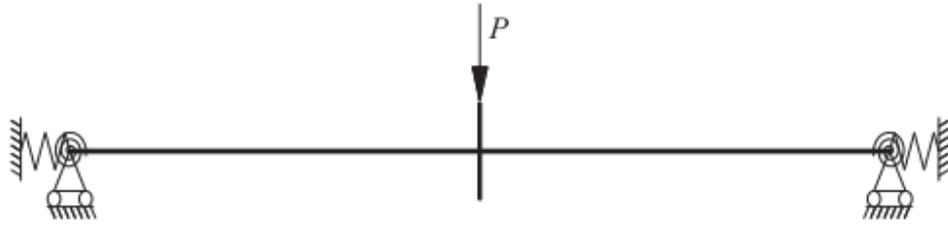
**Fig. 15.** Simplified mechanical model.

a) Elastic stage

b) Elastic-plastic stage

c) Arch stage and plastic stage

d) Transient stage and catenary stage

e) Arch model

f) Arch model with springs
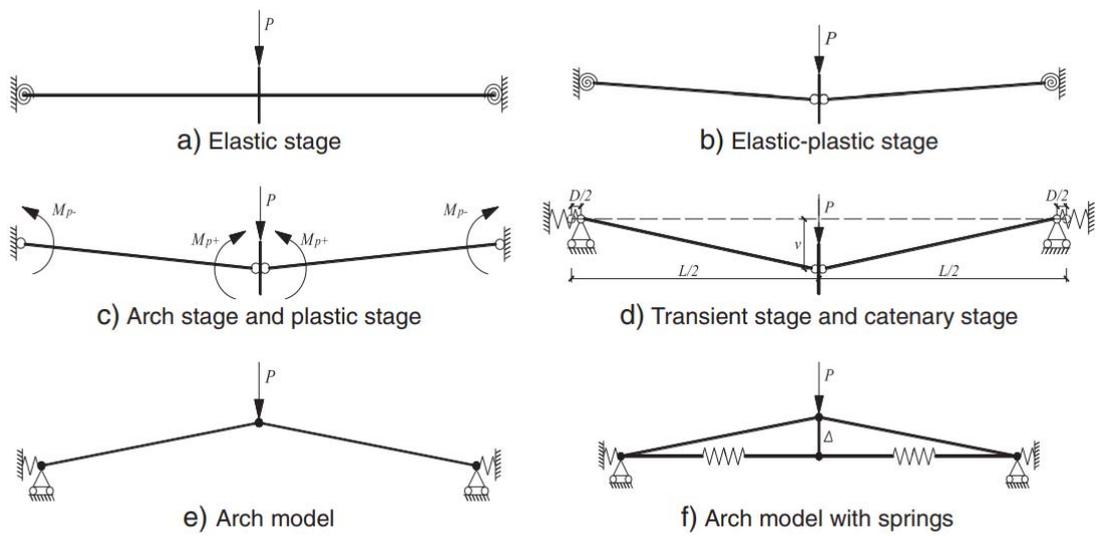
Fig. 16. Mechanics model in different stages.

Column C

Column D

Column E
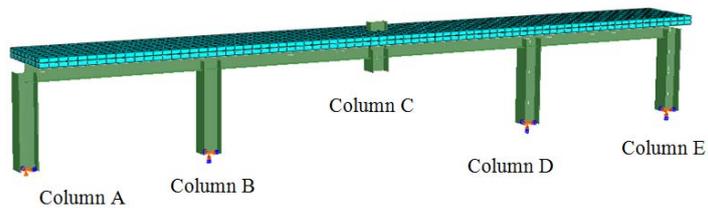
Column A

Column B

Fig. 17 The FE model
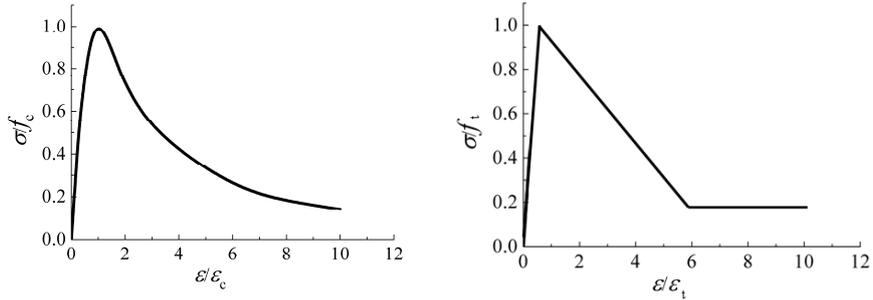
(a) Compressive relationship   (b) Tensile relationship

Fig. 18 Stress-strain relationship of concrete
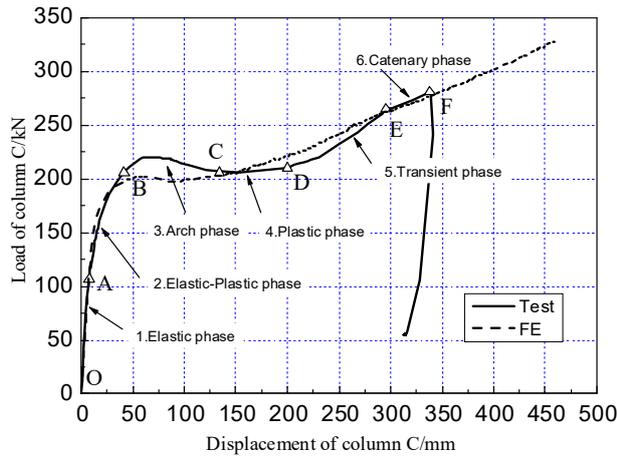
Fig. 19 Vertical load vs. displacement of middle column relationship curve

Table 1 Mechanical properties of steel

Se.		f_y（MPa）	f_u（MPa）	E_s（10^5MPa）
Beam	Flange	269	401	1.96
	Web	275	411	2.09
Column	Flange	247	396	2.00
	Web	276	415	1.98
Reinforcement	Φ8	325	487	-
	Φ12	331	464	1.95
Grade 10.9 bolt	Φ16	1067.4	1186	2.00

Table 2 Detailed results of test and simulation

	Initial stiffness (kN/mm)	Plastic resistance (kN)	Plastic displacement (mm)	Stiffness in catenary phase (kN/mm)
Test	16.0	206.7	41.5	0.397
Simulation	15.5	198.7	43.7	0.408